Agrobacterium rubi^T DSM 6772 Produces a Lipophilic Polysaccharide Capsule whose Degree of Acetylation is Growth Modulated

Cristina De Castro,* Valentina Gargiulo, Rosa Lanzetta, and Michelangelo Parrilli

Department of Organic Chemistry and Biochemistry, University of Naples, Complesso Universitario Monte Sant' Angelo, Via Cintia 4, 80126 Napoli, Italy

Received November 14, 2006; Revised Manuscript Received December 22, 2006

The structure of the capsular polysaccharide produced from the type strain of *Agrobacterium rubi* DSM 6772 is demonstrated by means of chemical and spectroscopical methodologies. It is constituted from the quite rare monosaccharide 6-deoxy-L-talose, involved in alternating α-(1 → 2) and α-(1 → 3) linkages. This simple backbone is further complicated from the occurrence of *O*-acetyl substituents located always at *O*-2 of the *O*-3 substituted 6-deoxy-talose. This decoration is not stoichiometric and it depends on the growth stadium of the bacterium, leading to an almost regular acetylation pattern only at the stationary phase, where all the potential positions are substituted.

Introduction

Agrobacterium rubi is a Gram-negative bacterium, able to infect a broad range of dicots, although it shows an enhanced preference for plants belonging to *rubus* genus, like strawberries, blackberries, and so forth. Its mode of action is similar to that of *Agrobacterium tumefaciens*, and it is connected to the Ti plasmid, responsible for its phytopathogenic activity that culminates with the integration into the plant genome of a segment termed T-DNA. The mutated guest acquires the ability to produce a different range of opines, the *Agrobacterium*'s nutrients, and this mutation is accompanied by a second but more subtle one responsible for the production of phytohormones that promote the cell-uncontrolled growth and the consequent formation of the so-called crown-gall tumor.

In the case of the closely related *A. tumefaciens*, the genetic mechanism underlying the development of the disease is quite well established, but the events preliminary to this genetic material transfer are not completely elucidated, although they are fundamental for the plant−microbe interaction establishment. Several reports point to the external membrane molecular components[1] attributing to them an important role in the adhesion process among the bacterium and the plant cell wall; these components are represented from lipopolysaccharides (LPS), proteins, exocellular (EPS), and capsular polysaccharides (CPS).

Interestingly, these last two macromolecules are not always produced from the bacterium, but when present, they do not share the same functions, the same physical location, or the same structure; exopolysaccharides are usually secreted in the growing medium whereas the capsular polysaccharides coat tightly the bacterial external membrane.

To date, many data describing the structure/biological activity relationship of EPS are available for the phylogenetically related *Rhizobium* genus, proving that these macromolecules are deeply involved at the early stages of the symbiosis establishment.[2] Similarly, the capsular polysaccharides add some additional features, as demonstrated for *Sinorhizobium meliloti*, where it was proved that the CPS acts in two ways: one active in the plant−bacterium signaling and one passive, that is, the masking of the bacterium from the defense products of the plant or from other microbial sources.

In this context, data regarding the structure of exocellular or capsular polysaccharides from *Agrobacterium* genus are very poor, although the information available show that they share with *Rhizobium* the presence of acidic residues, like uronic acids or ketals of pyruvic acid.[3] In the case of *A. rubi* DSM 6772, different from the data reported so far for the other *Rhizobiaceae*, the occurrence of a neutral, rather lipophilic, CPS is demonstrated; in addition, this polysaccharide is decorated with *O*-acetyl groups, whose substitution pattern is modulated during the growth stadium of the organism.

Experimental Section

Bacterial Cell Growth. *Agrobacterium rubi* strain DSM 6772 (type strain) was grown, in sterile conditions, at 27 °C in liquid shaking culture (120 rpm) in nutrient broth (Fluka Nutrient Broth No 4 cod. 03856). Typically, colonies grown on nutrient agar (DIFCO 269100) were transferred into the liquid medium and were monitored until the suspension reached an OD_{600} equal to 0.400, and the solution was added to 100-fold excess of fresh medium; in these conditions, the bacterium started the LOG phase after 14 h and reached the stationary phase after 36 h.

These growing parameters were used to collect the biomass at the end of the LAG period (14 h), at the middle exponential phase (after ca. 25 h), or at the stationary phase (44 h); in each case, the bacterial suspension was centrifuged (6000*g*, 10 min), and harvested cells were washed sequentially with 0.85% aqueous NaCl, ethanol, acetone, and diethyl ether and were freeze-dried yielding 2.5, 65, and 110 mg L^{-1} of dry cells, respectively.

Isolation and Purification of the Capsular Polysaccharide. Dried cells were extracted according to the hot phenol−water method,[5] and both phases were extensively dialyzed, freeze-dried, and monitored for carbohydrate components by SDS PAGE (sodium dodecyl sulfate polyacrylamide gel electrophoresis) and chemical analysis.

Discontinuous SDS PAGE[6] was performed with a 12% acrylamide separating gel on a miniprotean gel system (Bio-Rad). The samples

* Author to whom correspondence should be addressed. Phone: +39081674124. Fax: +39081674393. E-mail: decastro@unina.it.

10.1021/bm061081f CCC: $37.00
Published on Web 02/07/2007

were run at constant voltage (150 V) and were stained with silver nitrate according to the procedure of Kittelberger and Hilbink.[7]

Size exclusion chromatography was performed with Sephacryl HR-500 as adsorbent (Amersham-Biosciences, column 1.5 i.d. × 90 cm, eluent NH_4HCO_3 50 mM, flow 0.4 mL/min), and the eluate was monitored with a refractive index refractometer (K-2310 Knauer).

General and Analytical Methods. Monosaccharides were analyzed as *O*-acetylated methyl glycoside derivatives and fatty acids as methyl esters, as reported.[8] Glycosyl-linkage analysis of CPS was performed according to the procedure of Sandford and Conrad,[9] and the permethylated polysaccharide was recovered in the organic layer of the water/chloroform extraction and was converted in its partially methylated alditol acetates.[10]

GC-MS analysis conditions for all derivatives mentioned were the same as reported[8] but in the case of the acetylated glycosides were adjusted for glycerol detection using the temperature program 80 °C for 5 min, 80 → 300 °C at 10.0 °C/min, and 300 °C for 3 min with a solvent delay of 10 min on an Agilent 5973 instrument, using a SPB-5 capillary column (Supelco, 30 m × 0.25 i.d. flow rate, 0.8 mL/min; He as carrier gas).

Isolation of *O*-Methyl-α-L-6-deoxy-talopyranoside. Capsular polysaccharide (2 mg), dried over P_2O_5 in a desiccator, was treated with 1 M methanolic HCl at 80 °C for 2 h; lipids were removed by repeated extractions with *n*-hexane, and hydrochloric acid and methanol were removed by evaporation with a stream of air leading to a methylglycoside mixture that was further purified by RP-18 column on an HPLC system (Agilent series 1100, mq water as eluent at 0.8 mL/min, equipped with an R.I. detector). In these conditions, *O*-methyl-α-L-6-deoxy-talopyranoside was eluted at 30 min.

L configuration of 6d-talose derivative was deduced by the comparison of its optical rotation ($c = 0.2$, $[\alpha]_D = -117°$) with that reported in literature ($c = 2.1$, $[\alpha]_D = -104°$).

NMR Spectra Acquisition. Homonuclear ($^1H-^1H$) and heteronuclear ($^1H-^{13}C$) 2D-NMR experiments were carried out at 25 °C on a Varian Inova 500 of Consortium INCA (L488/92, Cluster 11), equipped with reverse probe. Chemical shift of spectra recorded in D_2O are expressed in ppm relative to internal acetone (2.225 and 31.4 ppm). Two-dimensional spectra (DQ-COSY, TOCSY, NOESY gradient-HSQC) were measured using standard Varian software.

For the homonuclear experiments, 512 free induction decays (FIDs) of 2048 complex data points were collected, with 40 scans per FID. The spectral width was set to 10 ppm and the frequency carrier was placed at the residual water signal. Mixing times of 120 and 200 ms were used during the acquisition of TOCSY and NOESY spectra, respectively. For the HSQC spectrum, 256 FIDS of 2048 complex points were acquired with 50 scans per FID, and the GARP sequence was used for ^{13}C decoupling during acquisition. Conversion of the Varian data, processing, and analysis were performed with Bruker Topspin 1.3 program.

Molecular Mechanics and Dynamics Calculations. Molecular mechanics calculations were performed using the MM3* force field as implemented in MACROMODEL 8.0, installed under Red Hat Enterprise operative system. For the glycosidic linkage, Φ is defined as $H_1-C_1-O-C_{aglycon}$ and Ψ as $C_1-O-C_{aglycon}-H_{aglycon}$. The calculations were performed with dielectric constant $\epsilon = 80$ as an approximation for bulk water. Energy map was calculated for the selected disaccharide employing the DRIV utility (with the DEBG option 150 of the program)[11] and was visualized with the 2D-plot facility of the program. In the DRIV option, both Φ and Ψ were varied incrementally using a grid step of 18°, and each (Φ, Ψ) point of the map was optimized using 1000 P.R. conjugate gradient.[12]

Probability distributions were calculated for each Φ, Ψ point according to a Boltzmann function at 298 K, and ensemble-average distances between intra- and inter-residue proton pairs were calculated as reported.[13]

Table 1. 500 MHz, 25 °C, ^1H and ^{13}C (Italics) Chemical Shifts of the Capsular Polysaccharide from *A. rubi* Strain 6772 Collected at the Stationary Phase[a]

residue	1	2	3	4	5	6
A	5.20	4.00	4.15	3.75	4.17	1.27
2)-6d-tal-(1 →	*99.2*	*80.0*	*67.6*	*73.5*	*69.6*	*17.5*
B	5.16	3.94	3.96	3.72	4.06	1.27
2)-6d-tal-(1 →	*99.7*	*80.0*	*69.5*	*73.3*	*69.8*	*17.5*
C	5.08	4.06	3.98	3.94	4.11[b]	1.27
3)-6d-tal-(1 →	*105.6*	*71.1*	*72.9*	*71.1*	*69.5*[b]	*1.27*
D	5.06	5.24	4.22	3.95	4.14	1.27
3)-6d-tal-(1 →	*102.9*	*71.4*	*72.2*	*69.5*	*69.8*	*17.5*

[a] 6d-tal = 6-deoxy-talose. [b] These signals were not determined initially because of their low abundance and the coincidence with the intense H-5 and C-5 signals of **D**. Their chemical shift is based on the values found for the homologous residue of the polysaccharide from the bacterium grown at the middle of the LOG phase.

Results and Discussion

Capsular Polysaccharide Isolated from the Stationary Phase Growth. Capsular polysaccharide was isolated in the phenol layer of the hot water/phenol extract of the dry cells, and it was further purified from proteic material by gel permeation chromatography using Sephacryl HR-500 as adsorbent, where it was eluted at 50% of the total column bed volume (yield 0.78%). Chemical analysis of the polysaccharide identified a main sugar component at 17.5 min, recognized as 6-deoxy-talose by comparison with an authentic standard, and other minor constituents: rhamnose (16.80 min) and glycerol (12.48 min). Kdo (23.32 min) was barely distinguishable in the baseline in agreement with the SDS-PAGE results showing a very weak staining in correspondence with low molecular weight lipopolysaccharide species (termed lipooligosaccharides or LOS). On the other hands, LOS fraction was partitioned in the water extract of the cells, and it displayed a different chemical composition (fucose, galacturonic and glucuronic acid, galactose, glucose, glucosamine, and Kdo) that lacked those residues associated to the CPS, rhamnose and 6-deoxy-talose.

Methylation analysis of the CPS defined the substitution pattern of both 6-deoxy-talose and rhamnose; the first residue was either 2-*O* or 3-*O* substituted while the second was found only *O*-3 substituted.

Fatty acid pattern differed from that reported for *Agrobacteria* LOS[14] for the absence of hydroxyl-bearing species and that were replaced instead from the unsatured fatty acid C18:1[9] as main constituent together with C16:1,[9] C 16:0, C 18:0, and C19:0.

NMR spectroscopic analysis (Table 1) led to the complete elucidation of the polysaccharide structure. The anomeric region of the proton spectrum (Figure 1a) contained three main signals at 5.24, 5.16, and 5.06 ppm with similar proportions besides two other minor ones at 5.20 and 5.08 ppm; other diagnostic signals were present in the high-field region, namely, a methyl signal at 2.17 ppm, belonging to an acetyl group and two doublets at ca. 1.3 ppm arising from the H-6 methyl signals of two 6-deoxy-talose residues.

Analysis of the HSQC spectrum revealed that the signal at 5.24 ppm was a proton geminal to an *O*-acetyl group, shifted in that region from the electron-withdrawing substituent. The anomeric protons were labeled with a capital letter, and the approach discussed here for residue **D** was applied to all other units, leading to the determination of the primary structure of the polymer. The low-field proton at 5.24 ppm was attributed as H-2 of residue **D** as demonstrated from the pertinent H-2/H-1 correlation in the COSY spectrum. In addition to this cross-

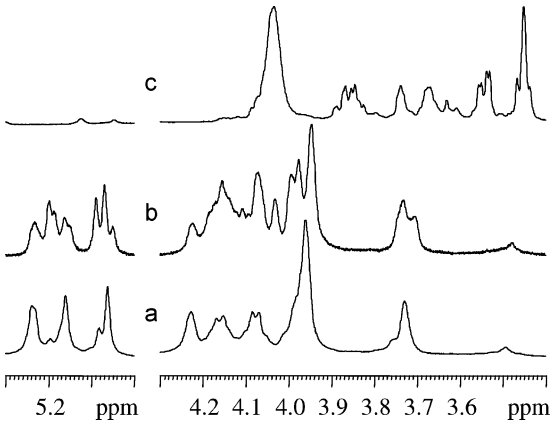

Figure 1. (500 MHz, 25 °C) Proton spectra of products isolated in the phenol layer of the hot phenol/water extraction of *Agrobacterium rubi* DSM 6772 at three different growth stages: (a) stationary phase, (b) middle exponential phase, and (c) late LAG phase.

peak, H-2 showed two other cross correlations, one with H-3 and another much less intense with H-4, originated from the "W" arrangement linking these two protons in the *talo* configured sugars. Proton H-4 did not correlate with proton H-5 because of the small coupling dictated from the *syn* orientation between them. H-5 signal was identified on the basis of two intraresidue NOE effects, one of medium intensity with H-3 and a stronger one with H-4; H-5/H-6 correlation was instead visible in the COSY spectrum. Clearly, the H-2/H-4 W-coupling, together with the lack of the H-4/H-5 correlation in the COSY spectrum, confirmed the *talo* configuration of the residue inspected.

The complete elucidation of the HSQC spectrum presented some ambiguities in the region at 3.95 ppm because of the overlapping of two signals, H-2 of **B** and H-4 of **D**. The correct attribution was possible taking into account the methylation data, according to which no residue was substituted at position *O*-4. On this basis, the carbon signal at higher field, 69.5 ppm, was assigned as at *C*-4 of **D** and the other, shifted at low field with respect to the standard value[15] because of the α-glycosylation effect, was instead *C*-2 of **B**. On the basis of the carbon chemical shift assignments, unit **D** was the one glycosylated at *O*-3 whereas unit **B** was *O*-2 substituted. The sequence establishment was confirmed from the NOESY spectrum that showed an intense correlation among H-1 of **B** and H-3 of **D** and the other expected between H-1 of **D** and H-2 of **B**. These NOE data rule out the existence of two different homopolymers, one assembled only with *O*-2 linked 6-deoxy-talose units and the other with only *O*-3 substituted 6-deoxy-talose units.

For the two minor signals, **A** and **C**, attributed in a similar fashion, residue **A** was an *O*-2 linked 6-deoxy-talose unit, but differently from **B**, it was connected at *O*-3 of the nonacetylated residue **C**.

The α configuration at both anomeric centers was deduced from the same $^1J_{C,H}$ value of 173 Hz, measured by an HSQC without decoupling during the acquisition period.

Spectrum analysis showed that the capsular polysaccharide possessed a rather regular repeating unit, composed from residues **B** and **D** and represented in structure **1** (Figure 2), beside a second one that differed from the previous being not acetylated at position *O*-2 of the *O*-3 linked 6d-tal unit (Figure 2, structure **2**, residues **A** and **C**).

Capsular Polysaccharide Isolated from the Middle Exponential Phase Growth. Application of the same purification protocol led to the purification of the CPS (yield 1%) whose chemical composition was in agreement with that found in the previous case. Despite the chemical identity, the appearance of the proton spectrum of this polysaccharide (Figure 1b) was different in that its anomeric region was crowded and displayed eight signals with no apparent stoichiometric ratio.

Analysis of the anomeric region of the HSQC spectrum showed that the broad signal at lower field was due to a hydroxy-methylene proton, shifted by acetylation; on the other hand, the remaining seven signals counted for a total of eight anomeric protons, two of them being overlapped in the proton spectrum but resolved in the carbon dimension. In addition, the lowest field signal was composed from two distinct carbinolic protons as visible from the COSY cross-peaks relating this signal to two different anomeric protons, namely, H-1 of **G** and **D**. The complete attribution of all the proton resonances was achieved combining the information from both COSY and TOCSY spectra (Table 2). This last was particularly valuable (Figure 3) in the assignment process, because starting from each anomeric signal, it reported the chemical shifts of the first four protons within the same sugar ring, whose correct sequence identification was ascertained combining the COSY spectrum data, whereas assignment of H-5 for each residue followed the NOESY spectrum interpretation as described above for the polysaccharide isolated at the stationary phase.

The sequence among all the residues was deduced from the inter-residue NOE effects, and in particular, the following effects (Figure 4) were relevant and resolved immediately part of the sequence attribution: H-1 of **A** with H-3 of **C**, H-1 of **C** with H-2 of **A**, H-1 of **B** with H-3 of **D**, H-1 of **D** with H-2 of **B**, and H-1 of **E** with H-3 of **G**.

The first two couples of NOEs were diagnostic of the two structural patterns already described for the stationary phase CPS, depicted from structures **2** and **1** (Figure 2), whereas the fifth NOE listed belonged to a new structural element absent in the previous polymer.

Attribution of NOEs from residues **H**, **F**, and **G** instead suffered from the overlapping of some key resonances, namely, H-1 of **H** showed intense NOE with a signal at 3.99 ppm where both its H-2 and H-3 of **F** were present. Similarly starting from the coincident anomeric protons of **F** and **G**, some NOEs involving H-2 of **E** and H-2 of **H** were clearly visible, but their correct attribution to either **F** or **G** was not possible at this stage.

Resolving information were obtained from the interpretation of all the NOEs from residue **E**, and actually this unit was *O*-2 substituted and was placed at the *O*-3 position of **G** by virtue of the inter-residual NOE effect; moreover, its anomeric proton showed a second weak correlation with a signal at 4.11 ppm, where H-5 of both **F** and **C** resonated. Since **C** was already located in another structural motif (Figure 2, structure **2**), this NOE was attributed to H-5 of **F** and it was explained by computer simulation of the disaccharide **3** (Figure 2): α-L-6d-tal-(1 → 2)-α-L-6d-tal, where the reducing unit in bold represents unit **E**, and the other is its *O*-2 substituent, namely, **F**.

The molecular mechanics approach was selected to evaluate the optimal dihedral angles Φ and Ψ of the glycosidic junction of the disaccharide together with the distribution of all those conformers falling within an energy window of 20 kJ from the global minimum; this conformer population defined the three different minima displayed in the conformational map (Figure 5) and was used to simulate the NOE effects according to a full matrix relaxation approach. The simulated data confirmed the occurrence of a weak NOE effect between the anomeric proton of the reducing end of **3** with the H-5 of the residue

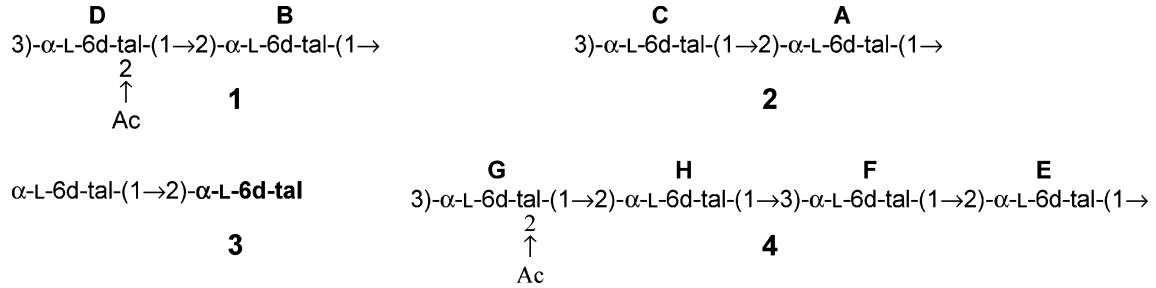

Figure 2. Structural motifs recognized in *A. rubi* DSM 6772 by means of NMR analysis. Structure **1**: defined from units **D**, **B**; all *O*-3 linked 6-deoxy-talose units are acetylated at *O*-2; main substitution pattern found in the stationary phase but less intense in the middle LOG growth of the bacterium. Structure **2**: defined from units **C**, **A**, deacetylated polymer found in traces at the stationary phase but is prominent at the middle LOG. Structure **3**: disaccharide elaborated for the simulation of the experimental NOEs found for residue **E** (bold written and located in the reducing terminal) of the polymer isolated at the middle of the LOG phase. Structure **4**: tetrasaccharidic repeating unit produced only in the middle LOG phase growth; the acetyl substituent is located at *O*-2 of every second *O*-3 linked 6-deoxy-talose unit.

Table 2. 500 MHz, 25 °C, ^{1}H and ^{13}C (Italics) Chemical Shifts of the Capsular Polysaccharide from *A. rubi* Strain 6772 Collected at the Middle of the Exponential Phase[a]

residue	1	2	3	4	5	6
A	5.20	4.03	4.16	3.73	4.18	1.27
2)-6d-tal-(1→	*98.4*	*79.1*	*66.7*	*72.9*	*68.8*	*17.5*
B	5.15	3.95	3.96	3.72	4.07	1.26
2)-6d-tal-(1→	*98.7*	*79.0*	*66.6*	*72.6*	*69.1*	*17.5*
C	5.09	4.08	3.99	3.95	4.11	1.28
3)-6d-tal-(1→	*104.7*	*70.3*	*72.1*	*70.2*	*69.5*	*17.5*
D	5.05	5.23	4.22	3.95	4.15	1.28
3)-6d-tal-(1→	*102.9*	*70.6*	*71.4*	*70.2*	*68.8*	*17.5*
E	5.16	3.98	3.98	3.71	4.07	1.26
2)-6d-tal-(1→	*98.7*	*79.0*	*66.6*	*72.7*	*69.1*	*17.5*
F	5.07	4.06	3.98	3.94	4.11	1.28
3)-6d-tal-(1→	*104.7*	*70.3*	*72.1*	*70.2*	*69.5*	*17.5*
G	5.7	5.24	4.23	3.95	4.164	1.28
3)-6d-tal-(1→	*102.9*	*70.6*	*71.4*	*70.2*	*68.8*	*17.5*
H	5.19	4.00	4.14	3.75	4.18	1.27
2)-6d-tal-(1→	*98.4*	*79.1*	*66.7*	*72.6*	*68.8*	*17.5*

[a] 6d-tal = 6-deoxy-talose.

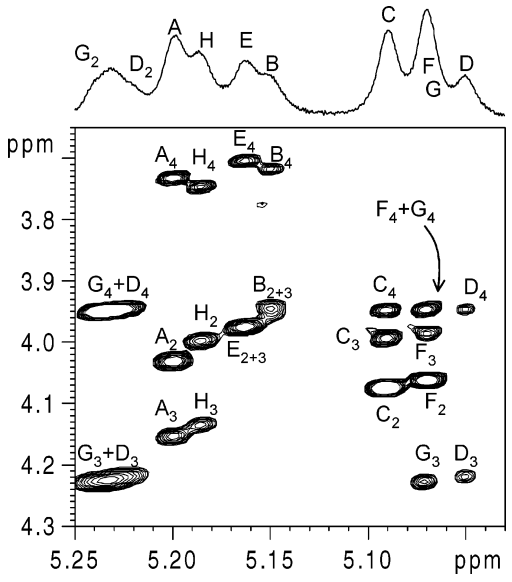

Figure 3. (500 MHz, 25 °C) Density attribution of the anomeric area of TOCSY spectrum of capsular polysaccharide isolated at the middle of the LOG phase growth.

placed at its *O*-2. Moreover, this result clarified the occurrence of other NOEs in the NOESY spectrum: H-1 of **A** with H-5 of **C**, H-1 of **B** with H-5 of **D**, and H-1 of **H** with H-5 of **G**.

On the basis of the above results, the sequence **F**-**E**-**G** was

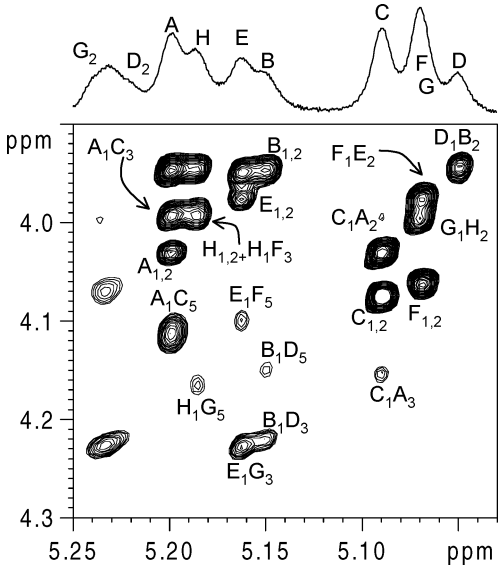

Figure 4. (500 MHz, 25 °C) Anomeric area of NOESY spectrum of capsular polysaccharide isolated at the middle of the LOG phase growth. More relevant effects are marked on the spectrum.

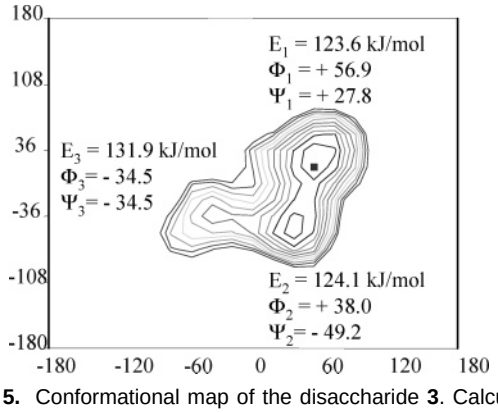

Figure 5. Conformational map of the disaccharide **3**. Calculations were performed with MM3 force field with dielectric constant $\epsilon = 80$ as implemented in MacroModel 8.0. Three different minima were found as indicated on the graphic.

inferred and further elongated with one sugar residue because of the NOE occurring between H-5 of **G** and H-1 of **H**, leading to the elaboration of structure 4 (Figure 2).

Consequently, the NOE effects seen for the overlapping anomeric protons **F** and **G** were assigned as follows: H-1 of **F** with H-2 of **E** and H-1 of **G** with H-2 of **H**. The new sequence established (structure **4**, Figure 2) was characterized again from a backbone with alternating *O*-3 and *O*-2 6-deoxy-talose residues but with acetylation pattern different from that of structure **1**

(Figure 2), with this decoration now being located every second *O*-3 linked sugar unit.

Material Isolated from the Late LAG Phase Growth. Dry cells were extracted in the conditions for capsular polysaccharide isolation, and 6-deoxy-talan derivative was not found in detectable amounts. The whole procedure led to the isolation of a different product shown in the proton spectrum (Figure 1c) that was not further studied (2 mg, yield 10%).

Conclusions

Agrobacterium rubi DSM 6772 produces a capsular polysaccharide composed from the uncommon sugar, the 6-deoxy-L-talose. The classification of this polysaccharide as capsular follows several considerations. First, it was never found in the growth medium (data not shown), and it could be detached from the cell wall only after the strong denaturing method of the hot water−phenol extraction, suggesting its anchoring on the bacterial membrane. In addition to this, it did not contain those components retained as markers of lipopolysaccharides, namely, Kdo and 3-hydroxy fatty acids, and it did not appear on SDS-PAGE as instead usually happens for LOS molecules. On the other hand, the presence of glycerol and long-chain, not hydroxylated, fatty acids is consistent with data referring to other bacteria[16] that reports the anchoring of these molecules to the membrane through a unit of 2,3-diacyl phospho-glycerol; any attempt to detect phosphorus or glycerol by NMR measurement failed (data not shown) probably because of their low amount in the sample. Similarly, the rhamnose unit, apparently associated to this polysaccharide, could not be located since it could never be identified in the NMR spectra.

Another important feature is the growing modulated structure of the polymer. Actually, it is not produced in the early stage of the bacterium life, in agreement with its nonvital role for the viability of the bacterium, whereas it is present when *A. rubi* reaches a sensible concentration in the growing medium, suggesting that modulation of its synthesis responds to the quorum-sensing regime establishment as described for other bacterial species.

Similarly, the acetylation pattern is growth dependent and the substituents are always located at *O*-2 position of an *O*-3 substituted 6-deoxy-talose unit, generating the three different motifs described in the CPS isolated at the middle of the LOG phase, in which the acetyl is never or always present or is located every second potential residue (Figure 2, structures **2**, **1**, or **4**, respectively). The occurrence of these three different structural motifs deserves a clarification. Actually, the hypothesis of three distinct polymers is very unlikely whereas the most plausible structural model figures the presence of different domains within the same polysaccharide chain, with each domain decorated according to one of the motifs found by NMR spectroscopy analysis.

This apparent heterogeneity in the substitution modality disappears in the polymer isolated in the stationary phase, where almost all the potential acetylation sites are occupied from the substituent, leading to the observation of a nearly regular structure.

From these experimental results, it appears that the acetyl substitution is delayed with respect to the polysaccharide production, reaching the completeness only at the late growth stage. The need for an extensive acetylation of the capsular polysaccharide might be related to the enhanced hydrophobicity displayed from the polymer that might play a key role in the adhesion properties of the bacterium in the context of the plant wound areas colonization or of a performing biofilm structuring.

Acknowledgment. The authors thank the "Centro di Metodologie Chimico-Fisiche" of the University Federico II of Naples for NMR facilities and thank PRIN 2004 (M. P.) for financial support. C. D. expresses her sincere thanks to Andreas Baier (student inside the Leonardo training program) for his help in the chemical analysis of the CPS.

References and Notes

(1) Matthysse, A. G. *CRC Crit. Rev. Microbiol.* **1986**, *13*, 281.
(2) Fraysse, N.; Courdec, F.; Poinsot, V. *Eur. J. Biochem.* **2003**, *270*, 1365.
(3) Bradley, R. L.; Kim, J. S.; Matthysse, A. G. *J. Bacteriol.* **1997**, *179*, 5372.
(4) Evans, R. L.; Linker, A.; Impallomeni, G. *Int. J. Biol. Macromol.* **2000**, *27*, 319.
(5) Westphal, O.; Jann, K. *Meth. Carbohydr. Chem.* **1965**, *5*, 83.
(6) Laemmli, U. K. *Nature (London)* **1970**, *97*, 620.
(7) Kittelberger, R.; Hilbink, F. *J. Biochem. Biophys. Methods* **1993**, *26*, 81.
(8) De Castro, C.; De Castro, O.; Molinaro, A.; Parrilli, M. *Eur. J. Biochem.* **2002**, *269*, 2885.
(9) Sandford, P. A.; Conrad, H. E. *Biochemistry* **1966**, *5*, 1508.
(10) Albersheim, P.; Nevins, D. J.; English, P. D.; Karr, A. *Carbohydr. Res.* **1967**, *5*, 340.
(11) With DEBG 150, the DRIV option starts each incremental minimization from the initial structure as read from the input.dat file.
(12) Polak, E.; Ribiere, G. *Rev. Fr. Inf. Rech. Oper.* **1969**, *35*, 16−R1.
(13) Jimenez-Barbero, J.; De Castro, C.; Evidente, A.; Molinaro, A.; Parrilli, M.; Surico, G. *Eur. J. Org. Chem.* **2002**, *11*, 1770.
(14) Silipo, A.; De Castro, C.; Lanzetta, R.; Molinaro, A.; Parrilli, M. *Glycobiology* **2004**, 805.
(15) Zahringer, U.; Rettenmaier, H.; Moll, H.; Senchenkova, S. N.; Knirel, Y. A. *Carbohydr. Res.* **1997**, *300*, 143.
(16) Gotschlich, E. C.; Fraser, B. A.; Nimura, O.; Robbins, J. B.; Liu, T.-Y. *J. Biol. Chem.* 1981, **256**, 8915.

BM061081F